



Study of the incorporation of TMPyP and Rhodamine B into diphenylalanine peptide nanotubes

Bassel Alotibi^{1,2}, James Rice^{1*}

¹ School of Physics, University College Dublin

²Current affiliation: Teacher at the department of Education in Afif, Saudi Arabia

Corresponding author: Prof. James Rice Email: james.rice@ucd.ie Phone: +35317162229

Abstract: In this study we investigated Diphenylalanine (FF), which is well known to form complex self-assembled structures, including peptide microtubes, nanowires, and nanofibers, with morphologies depending on the amino (NH₃⁻) and carboxylic (COO⁻) terminal modifications. The aim of this study was to demonstrate whether fluorescent TMPyP and Rhodamine B are both noncovalently incorporated into FF peptide nanotubes (PNTs) during self-assembly when analyzed using spectroscopy and fluorescence methods.

Seven samples were prepared and analyzed for this experiment, including FF, TMPyP and Rhodamine B, either alone or in various combinations. Four techniques were employed to analyze the samples. UV-vis spectroscopy was conducted to identify and quantitate the molecules of interest in the solution. Fluorescence spectroscopy was conducted to measure total fluorescence in sample solutions and fluorescence microscopy established how much of the fluorophores were incorporated into FF micro/nanotubes during self-assembly. Lastly a Scanning Electron Microscope (SEM) was utilized to provide images of FF, TMPyP and Rhodamine B. Results obtained from this experiment showed that Rhodamine B was readily and stably incorporated into the walls of FF nanostructures, whereas TMPyP did not display as much affinity to FF micro/nanostructures as Rhodamine B. It is recommended that in future experiments, TMPyP samples be scanned using fluorescence microscopy at a different range (from 675 nm to 720 nm instead of at 420nm), in order to visualize how much reduced TMPyP is noncovalently incorporated into FF nanotubes.

Received: 1/1/2020
Accepted: 27/2/2020

keywords: Diphenylalanine (FF), peptide nanotubes, TMPyP, Rhodamine B

1. Introduction

1.1 General background

The term self-assembly can be explained in relation to Nano technology, whereby the objects, the devices, and also the systems autonomously form complex structures in response to detailed interactions amongst themselves [1].

The field of Nano-technology is one of the branches of engineering that focusses on designing, manufacturing, control the scale of a few nanometers (nm), where 1nm= 10⁻⁹ meter [2].

Regarding self-assembly, all the individual devices have within themselves information that is essential to create the template to form

the structures of multiple units. One such example is that the construction of the monolayer. In this process, the sole layer of the closely- arranged molecules is organized together on a surface in a logical and a closely packed pattern. Importantly, self-assembly should not be confused with positional assembly. This technique has been adopted to build objects, devices, and systems on a molecular scale. Positional assembly applies automated processes, whereby the components that are used to carry out the construction procedures can follow a programmed approach. The field of nanotechnology possesses potential advantages that can be utilized in many sectors, including; agricultural, water purification,

sanitation, and alternative energy (particular photovoltaic), residential and business construction, medicine, and computer manufacturing [3-8].

The present work responds to the following challenge, would it be possible to co-operate dyes inside the nanotube? This is a greater challenge in the field of self-assembly as unbalanced dye molecules have uncommon optical and electronic properties. A second challenge is whether the FF peptide nanotube, together with optically active molecules (TMPYP and Rhodamine B), lead to enhanced energy transfer. As such, we applied peptide nanotubes templates by adopting the two-molecule system, and studied the structure of the peptide Nano material, noticing whether the dye affected the peptide's structure and if the dyed peptides facilitated enhanced energy transfer.

1.2 Properties of Peptide Nano/ Micro-tubes

As discussed earlier, the field of self-assembly relates to Nanotechnology. As such, the properties of the peptides' Nano/Micro-tubes include microstructures that are biological in nature and possess intrinsic molecular recognition features that allow for extensive chemical and the conformational of the functional diversity. The other feature that these micro-tubes possess includes covalent bonding in varying degrees of PH concentration, in the form of the extracellular matrix protein elastin [9]. This protein is adaptable and allows for an extensive flexibility in both physical and chemical planes, making it an ideal compound to meet the diverse requirements of biomedical applications. In addition, binding to these micro tubes is dependent on the concentration [9]. All the morphological and the chemical changes are understood to complement the processes of self-assembly. The binding process of elastin can be examined by using an electron microscopic and other spectroscopic systems. An additional feature of micro tubes is that they have applications in ultra-precision devices. They are utilized primarily in the industrial environment. Areas where it is understood that any flaws will result in adverse outcomes. Microtubes are therefore critical in assisting the field of Biotechnology and can

make a mark on cutting edge technology [7,8,10].

1.3 Diphenylalanine (FF)

In the analysis of Diphenylalanine (FF), it has been discovered that nanostructures, especially those from peptide self-assemblies, have huge potential in their applications in the nanotemplating and nanotechnology fields [11, 12]. Previous exploratory studies reported that FF- based peptides could self-collect into exceeding specific nanostructures, for example, nanovesicles and nanotubes [13].

However, the atomic system of self-assembled nanostructures remains complicated. A portion of the study focusing on FF demonstrated the self-assembly pathways of 600 FF peptides at various fixations by performing broad coarse-grained atomic element (MD) reproductions [11]. In a range of forty 0.6–1.8 μ s directions at 310 K, starting from randomly assigned setups, FF dipeptides did not spontaneously form into circular vesicles and nanotubes, as expected. Instead, additional frames with new nano- structures, specifically, planar bilayers and a rich assortment of different states of vesicle-like structures (including toroid, ellipsoid, discoid, and pot-molded vesicles) were formed.

At low peptide fixations, the self-assembly included a combination of little vesicles and bilayers, whilst at high fixations, there was an initial arrangement in a bilayer, trailed by the bowing and conclusion in the bilayer. The development of various nanostructures could an aftereffect of the sensitive harmony amongst peptide peptide and peptide–water connections [11].

1.4 Forster Resonance Energy Transfer (FRET)

Forster Resonance Energy Transfer (FRET) is a distant-dependent tangible procedure in which the energy is transmitted nonradiatively from an excited molecular fluorophore (the donor) to another (the acceptor) employing means of intermolecular extended-range dipole-dipole coupling [14].

The hypothesis supporting energy exchange centers on the idea that the energized fluorophore is an oscillating dipole that can experience energy transfer with a second

dipole, which exhibits comparative reverberation recurrence [15]. As such, frequency energy exchange is undifferentiated from the conductivity of coupled oscillators. For example, two tuning forks vibrating at the same recurrence. Conversely, radiative energy exchange requires emission and reabsorption of a photon and relies upon the physical measurements, optical properties, geometry of the compartment, and the wave front pathways. Unlike radiative instruments, frequency energy exchange can yield substantial data concerning the benefactor acceptor pair. It is not sensitive to the encompassing dissolvable shell of a fluorophore, therefore when dissolvable ward occasions do occur, for example, fluorescence extinguishing, energized state responses, dissolvable unwinding, or anisotropic estimations, interesting questions arise.

The significant dissolvable effect on fluorophores required in reverberation vitality exchange is the impact on ghastry properties of the contributor and acceptor. Non-radiative energy exchange occurs over any separations longer than short-run dissolvable impacts. The dielectric way of constituents (dissolvable and host macromolecule) situated between the included fluorophores has almost no impact on the viability of frequency energy exchange, which depends principally on the separation between the contributor and acceptor fluorophore [16].

1.5 Application of FRET

FRET has been applied to calculate the distance between a fluorescence donor and acceptor that have suitably covering spectra. This strategy has been used to create separations between a fluorescence contributor arranged in a particular position inside a docked ligand and a fluorescence acceptor arranged in a clear position inside its receptor [17].

This strategy is relevant to receptor communication in the earth of an in place cell containing the full supplement of flagging and administrative proteins.

Various measurements are necessary, including; establishing the typical capacity of the adjusted ligand and receptor, ascertaining the nonattendance of vitality exchange to non-receptor proteins, and measuring the specificity

of exchange between the giver and acceptor of interest [18].

The aim of this study was to demonstrate, by means of several spectroscopy and microscopy methods, whether fluorescent TMPyP and Rhodamine B are noncovalently incorporated into FF PNTs during self-assembly.

2. EXPERIMENTAL METHODS

2.1 Sample preparation

Seven samples were prepared and analyzed in this experiment: FF; Rhodamine B; TMPyP; FF with Rhodamine B; FF with TMPyP; Rhodamine B and TMPyP together, and FF with both Rhodamine B and TMPyP. Both Rhodamine B and TMPyP solutions used for UV-vis spectroscopy, fluorescence spectroscopy and fluorescence microscopy, all at preparations of 50uM.

FF stock solution was prepared by dissolving 4 mg of lyophilized form of FF peptide monomer (Bachem AG) in 40 μ l 1,1,1,3,3,3-hexafluoro-2propanol (Sigma Aldrich) (10 mg/ μ l) and further diluted with 2ml ddH₂O to reach a concentration of 100 mg/ml. The stock solution was further diluted using deionized water to a final concentration of 2mg/ml. This was the concentration used for FF peptide nanotube (PNT) self-assembly.

In order to prepare the TMPyP (Frontier Scientific Inc.) stock solution, TMPyP was dissolved in ddH₂O to a final concentration of 50 μ M. Rhodamine B solution was also prepared at 10⁻⁵ M in water using the same method to prepare Tmpyp. The final volume was 31.

In order to demonstrate whether fluorescent cargos proteins were noncovalently conjugated into FF during self-assembly, the following combinations were prepared: FF/TMPyP/Rhodamine B mix was made by adding FF (1 mg/ml); TMPyP (250 ml of stock solution); and Rhodamine B (250 ml of stock solution) together in solution.

FF/TMPyP mix was made by adding FF (1 mg/ml) and TMPyP (250 ml of stock solution) together, FF/Rhodamine B mix by adding FF (1 mg/ml and Rhodamine B (250 ml of stock solution), and the TMPyP /Rhodamine B mix, by adding TMPyP (250 ml of stock solution)

and Rhodamine B (250 ml of stock solution) together.

2.2 UV-vis Spectroscopy

Absorption spectra of all samples were obtained using the Jasco v 650 UV-vis Spectrophotometer. An amount of 0.1 ml of freshly prepared sample solutions were placed in a 1 mm quartz cuvette and scanned individually from 200 to 800 nm. This included the UV and visible regions of the electromagnetic spectrum. The aim was to analyze and quantify the amount of substances of interest present in the solution.

In this case, λ_{max} of FF (280 nm), TMPyP (420 nm) and Rhodamine B (530 nm) were within the UV-visible region used, so they were anticipated to be detected. Also, dried FF annealed to the glass substrate was scanned to measure the amount of FF present at solid phase.

2.3 Fluorescence Spectroscopy

A second batch of fresh samples were prepared for fluorescence spectroscopy. 1 ml of each sample was mixed and pipetted into 1 mm quartz cuvette then placed into the light path of the fluorometer to measure total fluorescence of the sample solution. Total fluorescence of FF and fluorescent dyes, either alone or in combination, were measured at their corresponding known fluorescence excitation wavelengths. TMPyP was measured at 257 nm, Rhodamine B at 530 nm, and TMPyP at 420 nm respectively.

2.4 Fluorescence Microscopy

To prepare the samples for fluorescence microscopy, freshly prepared samples containing FF 100 μl of FF (1mg/ml) and 250 μl of fluorophore (1×10^{-5} M) were each pipetted into individual cover glass (Fig 3) and allowed to anneal onto the substrate through a process of evaporation at ambient conditions for one day. Slides containing air-dried samples were then placed and stabilized on the microscope stage and visualized using Zeiss Axio imager m1 john fluorescence imaging system.

Images were acquired using 10X, 20X and 40X objectives and FF nanotubes were visualized at 420 nm to display TMPyP

fluorescence and at 530 nm for Rhodamine B fluorescence.

Glass substrates containing the FF/TMPyP/Rhodamine B mixture were imaged before and after washing.

Washing was done by gently pipetting ddH₂O above the dried samples and left to soak for a day at ambient conditions before viewing.

3. Results

In this study, noncovalent intermolecular interaction of fluorescent dyes, Rhodamine B and TMPyP with L- diphenylalanine peptide nanotubes (FF-PNTs) were investigated using spectroscopic and fluorescence microscopy methods. The goal of this experiment was to demonstrate whether Rhodamine B or TMPyP were noncovalently incorporated, either alone or in combination, into FF-PNTs as L- diphenylalanine (FF) self-assembles into various nanostructures.

3.1 UV-vis Spectroscopy

UV-vis spectroscopy was conducted in order to detect the presence of FF and the two fluorophores, either alone or in combination, in experimental samples using the Jasco v 650 UV-vis Spectrophotometer (Fig 1). Samples were analyzed at UV (200-400 nm) and visible (400-800 nm) regions of the electromagnetic spectrum as the λ_{max} of these molecules were known. Spectroscopic results showed that the sample containing only FF generated a very robust and smooth peak at ~ 280 nm (Fig 1). The high absorbance value of roughly 3.4 can be accounted to the amount of FF that was used in the solution (2mg/ml) for FF-PNT self-assembly.

In comparison, samples containing both TMPyP and Rhodamine B displayed a jagged line, with three peaks (Fig 2).

One peak was observed at ~ 257 nm which could be a trace amount of FF contamination.

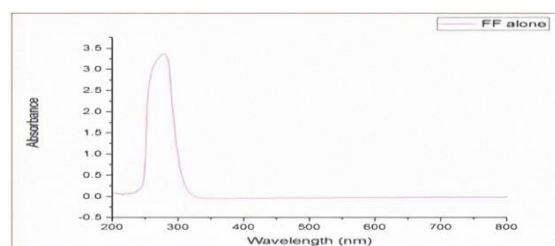


Fig 1. Absorption spectrum of diphenylalanine (FF) at 2mg/ml.

The other two peaks corresponded to the maxes of TMPyP (420 nm) and Rhodamine B (530 nm). The amount of fluorophores used (1×10^{-5} M) could be attributed to the smaller, less prominent peaks (0.14 - 0.15 Absorbance value) observed when compared to the FF peak.

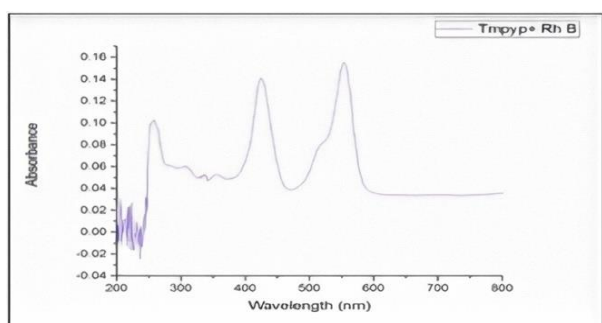


Fig 2. Absorption spectrum of TMPyP and Rhodamine B fluorophores (1×10^{-5} M).

Samples containing a combination of FF and each of the two fluorophores were also analyzed to test if FF exerted any effect that could interfere with the fluorescence of the fluorophore present in the mixture, or whether the presence of the fluorophore contained properties that could degrade or affect the absorbance of FF.

The resulting spectrographs of samples containing FF and TMPyP, and FF and Rhodamine B, showed peaks of FF and Rhodamine B at their respective λ_{max} (257 nm and 530 nm, respectively) consistent to the results when each fluorophore was analyzed alone.

Similarly, FF and TMPyP depicted the same pattern of absorbance peaks at their respective λ_{max} (257 nm and 420 nm, respectively), consistent with the results when each molecule was analyzed alone. These results indicated that FF did not interfere with the fluorescence of either Rhodamine or TMPyP, and that each dye did not degrade or affect the absorptive properties of FF when combined in solution. Therefore, both fluorescent dyes were efficient cargo indicators for FF-PNT studies.

The results also showed an absorption spectrograph of the sample containing all three molecules; FF, TMPyP and Rhodamine B in the mixture. The resulting spectrograph displayed a robust FF absorbance peak at λ_{max} , consistent with the λ_{max} of FF in other samples, whereas both Rhodamine B and TMPyP peaks were detectable at trace amounts

at their λ_{max} . This was consistent with the absorbance values of other samples containing dyes, either alone or in combination. The differences in the absorbance peaks between FF and the fluorophores was due to the amount of substance present in the samples being analyzed. Finally, UV-vis spectroscopy results generated consistent absorbance peaks for FF, TMPyP and Rhodamine B when analyzed alone or in combination, making this technique an efficient one in detecting the presence of molecules of interest.

3.2 Fluorescence Spectroscopy

The total fluorescence of sample solutions containing FF, TMPyP and Rhodamine B, either alone or in combination, was measured using a fluorometer (Photon Technology International).

Fluorescence peaks were observed in two regions when the solution containing FF alone was excited at 257 nm. The highest peak with a value of $\sim 49,000$ fluorescence units (FU) was observed at $\sim 280-300$ nm and a less prominent peak with a fluorescence value of almost 10,000 FU observable at ~ 555 nm. The appearance of the smaller peak could be attributed either to background fluorescence or trace contamination of Rhodamine B in the cuvette used.

Furthermore, Rhodamine B displayed a very smooth yet robust fluorescence peak (fluorescence value at 1.2 million FU) at $\sim 550-555$ nm, whereas TMPyP excited at 420 nm displayed a wider and flatter fluorescence peak with a fluorescence value of $\sim 75,000$ FU. This dramatically shifted to $\sim 675-730$ nm of the visible region. From these results, it is clear that Rhodamine B was a stronger fluorophore as it displayed the highest fluorescence signal compared to its weaker counterpart, TMPyP, when prepared either alone or in aqueous solution.

In order to investigate whether the fluorophores used affected the fluorescence intensities of the other and vice versa, fluorescence spectra of samples containing both fluorophores in solution were analyzed at 420 nm as well as 530 nm. There are the excitation wavelengths of Rhodamine B and TMPyP, respectively. Results indicated that when TMPyP/Rhodamine B mixture was excited at

420 nm, a wider fluorescence peak was observed (58,000 FU) from ~675 – 730 nm reminiscent of TMPyP fluorescence signature. However, the Rhodamine B signature fluorescence was not detectable at this wavelength.

When analyzed at 530 nm, Rhodamine B displayed a sharp peak with a value of ~610,000 FU, whereas TMPyP displayed a wider and shallower peak with a lower fluorescence value (~80,000 FU). This result indicated that fluorescent intensities of both fluorophores in a mixture had similar patterns compared to when each fluorophore was prepared alone in solution. This result agrees with previous findings, showing that Rhodamine B is a remarkably strong fluorescent dye when compared to TMPyP [18].

Total Fluorescence of FF and TMPyP mixture was also quantified using the excitation wavelength range of FF (257 nm and 300 nm) as well as at 420 nm which is the excitation wavelength of TMPyP. The results show a strong FF fluorescent peak at ~280-300 nm with a fluorescence value of ~12, 000 FU and a smaller peak (~3000 FU) at ~550-580 nm, reminiscent of the fluorescence bulge observed when FF was prepared alone in aqueous solution. This peak could either be some nonspecific background fluorescence or a trace Rhodamine B contamination in the cuvettes used. In addition, when analyzed at 300 nm, the FF/TMPyP mixture displayed a totally different fluorescence profile compared to the one displayed at 257 nm. Two distinct peaks were observed at 300 nm; the first peak at ~600 nm (~3100 FU) appeared sharper and steeper, whilst the peak at 675 – 720 nm was wide and flat (~3300 FU). Similarly, when the mixture was quantified at 420 nm, which is the excitation wavelength of TMPyP, two fluorescence peaks were also observed.

The first peak appeared steep and sharp at ~575 nm whereas a wider and flatter peak was observed at ~675 –720 nm. The fluorescence pattern at 420 nm was similar to the one observed when the mixture was analyzed at 300 nm but the peaks were not well defined.

The fluorescence spectrum was also obtained from the FF and Rhodamine B

mixture. Results illustrate the presence of two peaks at 257 nm; one at ~280 nm (~12, 000 FU), which could be attributed to the FF autofluorescence, while a higher and sharper peak at 575 nm could be accounted to the bright Rhodamine B fluorescence. This reached a value of ~36, 000 FU, corroborating previous results showing that Rhodamine B possesses a very strong fluorescence signal [19]. Additionally, when the mixture was analyzed at 300 nm, Rhodamine B fluorescence peak still remained intact at 575 nm displaying a fluorescence value of ~35,000 FU.

Since Rhodamine fluorescence can be readily detected at 300 nm, a sample solution containing FF, TMPyP and Rhodamine B mix were analyzed at 300 nm and 430 nm, in order to display both Rhodamine B and TMPyP fluorescence.

3.3 Fluorescence Microscopy

To demonstrate whether the fluorophores were in fact noncovalently conjugated into FFPNTs during self- assembly, the Zeiss Axio imager m1 john fluorescence microscope was used to visualize both TMPyP and Rhodamine B fluorescence, either alone or in combination, in FF PNTs. From the results generated, it appeared that Rhodamine B was successfully incorporated into FF tubes (Fig 3) especially into the walls of the hollow micro and nanotubes. Two types of fibers were observed; fine, fluorescent nanotubes/fibers, and larger, hollow fluorescent microtubes (Fig 3C and F). The patterns of fluorescence was mostly uniform along the span of the tubes. However, certain regions in some nanotubes displayed bright punctate fluorescence (Fig 3A and E), indicating that Rhodamine B had a higher affinity in certain areas of the FF peptide micro and nanotubes. One could argue that these regions of punctate fluorescence (Fig 3C and F) were points of overlap between micro/nanotubes, enhancing the fluorescence in these areas. However, Fig 3D shows the point of overlap among tubes without any noticeable spike in fluorescence.

TMPyP fluorescence in FF micro and nanotubes was also visualized using the Zeiss Axio imager m1 john with 20X objective and 40X objective. Unlike Rhodamine B staining, there was sparse distribution of TMPyP

staining in FF nanostructures when visualized at 490 - 560 nm. However, some TMPyP became readily incorporated into the walls of FF microtubes during self-assembly.

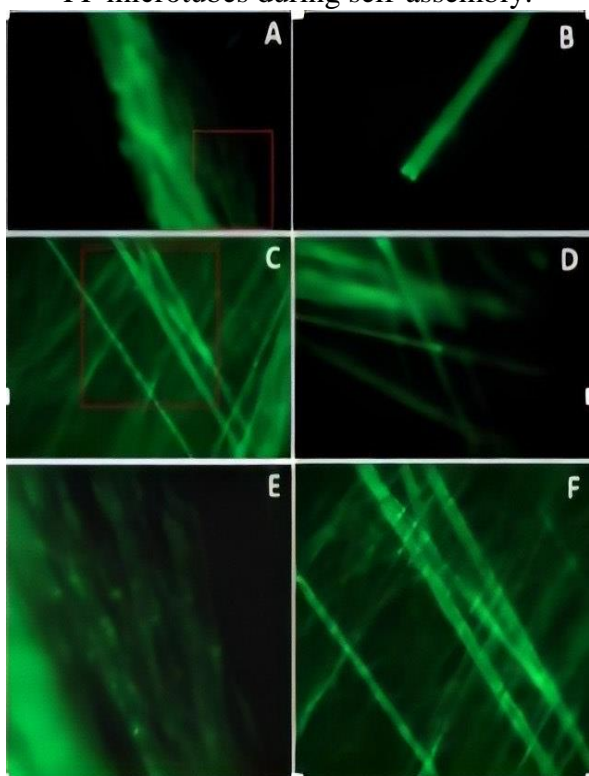


Fig 3. Fluorescence microscopy images of FF tubes stained with Rhodamine B acquired using Zeiss Axio imager ml john with 20X objective. FF micro and nanotubes are uniformly stained with Rhodamine B fluorescence (A, B, C, D, F). Bigger microtubes appear to be hollow with fluorescent staining only found on the walls of the tubes (C). D is the magnified field (highlighted in red) in C to emphasize FF nanostructures formed while E is the magnified region in A (highlighted in red) to emphasize regions of punctate fluorescence.

In order to demonstrate if the fluorophores were both incorporated into FF-PNTs during self-assembly, samples were visualized using 40X objective before and after washing. Results revealed that some FF tubes became fluorescent at 430 nm and 530 nm, indicating successful incorporation of both Rhodamine B and TMPyP into FF nanotubes. Before washing, more FF-PNTs were stained, compared to fluorescence images captured after the wash. Despite the decrease in abundance of stained nanotubes after washing (they may have been removed from the glass substrate), some FF micro/nanotubes appeared to be stained with both TMPyP and Rhodamine B dyes.

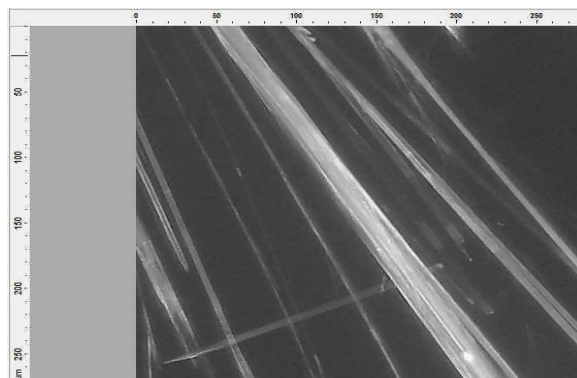


Fig 4 illustrates FF micro/nanotunes stained with TMPyP and Rhodamine B at 490 – 560 nm.

Fig 4. Fluorescence microscopy image of FF-PNTs stained with TMPyP and Rhodamine visualized at 490 to 560 nm.

3.4 Scanning Electron Microscope (SEM)

On a silicon substrate we scanned FF-PNTs (Fig 5A), FF-PNTs with TMPyP (Fig 5B), FF-PNTs with Rhodamine B at 5 μm (Fig 5C) and at 2.5 μm (Fig 5D).

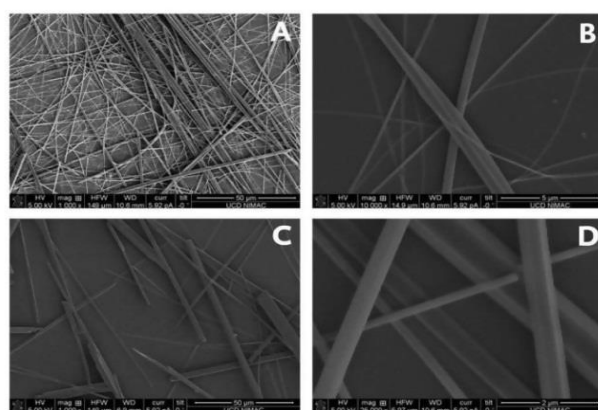


Fig 5: SEM images for A: FF-PNTs at 50 μm , **B:** FF-PNTs with tmpyp at 50 μm , **C:** FF-PNTs with Rodamine B at 5 μm and **D** FF-PNTs with Rodamine B at 2 μm .

4 Discussion

Several techniques were employed in this study in order to demonstrate intermolecular, noncovalent binding of TMPyP and/or Rhodamine B dyes into FF-PNTs during self-assembly at the liquid phase. UV-vis spectroscopy is a widely used characterization tool used to detect and quantitate the amount of molecules of interest in the solution. The Jasco Spectrophotometer we used in this study allowed for sufficient sensitivity in detecting molecules, or a mixture of molecules, in

solution. When both fluorophores were mixed with FF in aqueous solution, the UV-vis spectrophotometer generated sharp and accurate absorbance peaks of each molecule, regardless of whether the molecule was presented alone, or in combination with two fluorescent dyes. Absorbance spectrum obtained for each molecule displayed the λ_{max} of FF (280 nm), TMPyP (430 nm) and Rhodamine B (530 nm). λ_{max} of FF was reached at 280 nm. Maximum absorbance at this wavelength was attained by the presence of the aromatic rings in two of the phenylalanine residues that comprise FF. Furthermore, there were some discrepancies observed in the preparation of samples, especially in TMPyP/Rhodamine B mixture, where FF peak was also observed. This could be attributed to inefficient washing of cuvettes in-between readings, or there may have been some irregularities in the preparation of samples used for spectroscopy.

Although UV-vis spectroscopy is commonly used to quantify DNA, RNA and proteins, it can be unreliable and inaccurate at times. UV-absorbance is not selective and cannot distinguish DNA, RNA or proteins at 280 nm. Absorbance values are easily skewed by the presence of contaminants, free nucleotides, salts, and other compounds. Additionally, the sensitivity of spectrophotometry is often inadequate, prohibiting the quantitation of DNA at lower concentrations. Because of these shortcomings, the use of fluorescent dyes to quantitate nucleic acids and other molecules using fluorescence spectroscopy or fluorimetry became a more favored alternative. Fluorescence-based quantitation is more sensitive, and is more often specific to the fluorescent molecule of interest, when compared to UV-vis spectroscopy.

Although the amounts of FF, TMPyP and Rhodamine B were quantified using UV-vis spectroscopy, one cannot assume that all fluorophores present in the solution express fluorescence. Hence, the total fluorescence of sample solutions was quantified using a fluorometer (PTI). This measured the fluorescence intensities of the three chosen molecules when scanned at their known excitation wavelengths. Results indicate that even though the amounts of TMPyP and

Rhodamine B are the same (1×10^{-5} M), their fluorescence intensities in solution, either alone, or in combination, differs significantly. Rhodamine B expresses a significantly stronger fluorescence signal when analyzed at $\lambda_{exc} = 530$ nm compared to when TMPyP fluorescence was analyzed at $\lambda_{exc} = 430$ nm. The fluorescence signal of Rhodamine B is so strong that it is detectable at 257 nm and 300 nm, even though its excitation wavelength is at 530 nm. Surprisingly, Rhodamine B is not detectable at $\lambda_{exc} = 430$ nm, which is the excitation wavelength for TMPyP but is detectable at lower wavelengths (257, 300 nm). This result is also consistent with the results of fluorescence microscopy where Rhodamine B readily and stably bound to the walls of FF micro/nanotubes with great binding affinity. Conversely, a sparse fluorescence staining of FF nanotubes was observed when stained with TMPyP dye.

A number of scenarios are possible to explain the results. One likely explanation is that during FF/TMPyP assembly, TMPyP fluorescence at 430 nm is rapidly quenched due to electron charge transfer, which reduces TMPyP as an electron acceptor. This shifts its fluorescence peak from 420 nm to 675 nm to 720 nm after interacting with FF, which acts as the electron donor. In addition, this event may have happened prior to the samples were analyzed. Thus the majority of FF nanotubes appear to be unstained at 420 nm because presumably, their fluorescence had already shifted to 675- 720 nm. It is recommended that in future experiments, samples should be scanned from 675 nm to 720 nm using fluorescence microscopy in order to visualize how much reduced TMPyP is noncovalently incorporated into FF nanotubes. The second explanation is that it is also possible that TMPyP has lesser affinity to FF during self-assembly compared to Rhodamine B. This can also result in sparse TMPyP distribution in FF nanotubes. If this is the case, TMPyP staining needs to be optimized by increasing the amount of the fluorescent dye in the sample solution.

Albeit fluorescence spectroscopy is commonly used to measure total fluorescence of sample solutions, this technique is not able to demonstrate how much of these fluorescent dyes are in fact noncovalently conjugated to FF

micro/nanotubes. In order to visualize the incorporation of Rhodamine B and TMPyP into FF micro/nanotubes, the samples were visualized using fluorescence microscopy. Results obtained from this experiment showed that Rhodamine B is readily and stably incorporated into the walls of FF nanostructures, whereas TMPyP did not display as much affinity to FF micro/nanotubes as Rhodamine B. There is a sparse distribution of TMPyP along FF nanotubes, which strongly indicates either a low affinity to FF, or rapid quenching of TMPyP dye at 420 nm as it becomes reduced by the electron donor, FF further shifting its fluorescence emission of TMPyP to 675-720 nm. Another possibility is that perhaps less FF/TMPyP fibers are deposited onto the glass substrate which could also result in lower MPyP incorporation. Furthermore, It would also be extremely beneficial to this experiment to visualize FF nanotubes not only at 420 nm, but also at 675-720 nm, to demonstrate how much reduced TMPyP is incorporated into the walls of FF micro/nanotubes.

5. Conclusions

UV-vis spectroscopy generated consistent and accurate readings of λ_{max} of FF, TMPyP and Rhodamine B regardless of whether they were present alone or in a mixture with other fluorophores. The λ_{max} of FF can be seen at 280 nm, which could be accounted by the presence of aromatic rings in each of the two phenylalanine residues that make up FF. In addition, λ_{max} of TMPyP and Rhodamine B were also observed at 430 nm and 530 nm, respectively. Fluorescence spectroscopy or fluorometry showed a strong Rhodamine B signal at λ_{exc} = 530 nm. The signal was so strong that it was detectable even at 257 and 300 nm, wavelengths where FF absorbance/fluorescence is detected. Surprisingly, Rhodamine B was not detected at 420 nm but was at lower wavelengths (257 and 300 nm). Results of fluorescence spectroscopy are consistent with those of fluorescence microscopy, demonstrating that Rhodamine B readily and stably bound to the walls of FF micro/nanotubes, whereas TMPyP samples displayed relatively low fluorescence intensity as well as low affinity to FF micro/nanotubes, compared to Rhodamine B at λ_{exc} = 430 nm.

Using fluorescence microscopy we demonstrated that Rhodamine B is readily and stably bound to the walls of FF micro/nanotubes. Also, punctate fluorescence at certain regions of the FF tubes was observed, which strongly indicates that there are certain areas of the FF nanotube where Rhodamine B displays a higher affinity. For TMPyP staining, fluorescence images were obtained at λ_{exc} = 420 nm. TMPyP staining was observed to be sparsely distributed in the walls of FF nanotubes. This experiment however, did not examine FF/TMPyP or FF/TMPyP/Rhodamine B mixtures at 675-720 nm, which is the wavelength range for detection of the reduced form of TMPyP, as confirmed by fluorescence spectroscopy results. Taken altogether, further studies need to be done on TMPyP staining to include images acquired at 675- 720 nm in order to assess the level of reduced TMPyP present in FF nanotubes.

4. References

- 1 Drexler, K. Eric (1992). *Nanosystems: Molecular Machinery, Manufacturing, and Computation*. New York: John Wiley & Sons. ISBN 978-0-471-57547-4.
- 2- Allhoff, Fritz; Lin, Patrick; Moore, Daniel (2010). *What is nanotechnology and why does it matter?: from science to ethics*. John Wiley and Sons. pp. 3–5. ISBN 978-1-4051-7545-6.
- 3- Ariga, K., Hill, J. P., Lee, M. V., Vinu, Charvet, R., & Acharya, S. (2016). *Challenges and breakthroughs in recent research on self-assembly*. *Science and Technology of Advanced Materials*.
- 4 Au-Yeung, H. L., Leung, S. Y. L., Tam, A. Y. Y., & Yam, V. W. W. (2015). Correction to “Transformable Nanostructures of Platinum-Containing Organosilane Hybrids: Non-covalent Self-Assembly of Polyhedral Oligomeric Silsesquioxanes Assisted by Pt... Pt and π - π Stacking Interactions of Alkynylplatinum (II) Terpyridine Moieties”. *Journal of the American Chemical Society*, **137**(23), 7526-7526.
- 5 Azuri, I., Adler-Abramovich, L., Gazit, E., Hod, O., & Kronik, L. (2014). Why are diphenylalanine-based peptide nanostructures so rigid? Insights from first principles calculations. *Journal of the*

- American, Chemical Society*, **136(3)**, 963-969.
- 6 L. Liu, K. Busuttil, S. Zhang et al., (2011). "The role of self-assembling polypeptides in building nanomaterials," *Physical Chemistry Chemical Physics*, vol. **13**, no. 39, pp. 17435–17444,
 - 7 H. W. German, S. Uyaver, and U. H. E. Hansmann, "Self-assembly of phenylalanine-based molecules(2015) *The Journal of Physical Chemistry A*, vol. **119**, no. 9, pp. 1609–1615,
 - 8 C. H. Görbitz, (2006) "The structure of nanotubes formed by diphenylalanine, the core recognition motif of Alzheimer's β -amyloid polypeptide," *Chemical Communications*, no. 22, pp. 2332–2334, Nako Nakatsuka, Stacey N. Barnaby,
 - 9 Karl R. Fath & Ipsita A. Banerjee (2012) Fabrication of Collagen–Elastin-Bound Peptide Microtubes for Mammalian Cell Attachment, *Journal of Biomaterials Science, Polymer Edition*, **23**:14, 1843-1862, DOI: [10.1163/156856211X598229](https://doi.org/10.1163/156856211X598229)
 - 10 Prasad, S. K. (2008). *Modern Concepts in Nanotechnology*. Discovery Publishing House. pp. 31–32. ISBN 978-81-8356-296-6.
 - 11 Wegner, K. D., Jin, Z., Lindén, S., Jennings, T. L., & Hildebrandt, N. (2013). Quantum-dot-based forster resonance energy transfer immunoassay for sensitive clinical diagnostics of low-volume serum samples. *Acs Nano*, **7(8)**, 7411-74.
 - 12 Guo, Cong, et al. (2014): "Triphenylalanine peptides self-assemble into nanospheres and nanorods that are different from the nanovesicles and nanotubes formed by diphenylalanine peptides." *Nanoscale* 6.5 2800-2811.
 - 13 Acuna, Sergio M., et al. (2018). "Self-Assembly of Diphenylalanine-Based Nanostructures in Water and Electrolyte Solutions." *Journal of Nanomaterials*, vol. **2018**, Gale Academic OneFile, Accessed 20 Feb. 2020.
 - 14 Clegg, Robert (2009). "Förster resonance energy transfer—FRET: what is it, why do it, and how it's done". In Gadella, Theodorus W. J. (ed.). *FRET and FLIM Techniques. Laboratory Techniques in Biochemistry and Molecular Biology*. **33**. Elsevier. pp. 1–57. doi:10.1016/S0075-7535(08)00001-6
 - 15 Nelson PC. (2018) The Role of Quantum Decoherence in FRET. *Biophys J.*; **115(2)**:167–172. doi:10.1016/j.bpj.2018.01.010
 - 16 Qi, H., Ghodousi, M., Du, Y., Grun, C., Bae, H., Yin, P., & Khademhosseini, A. (2013). DNA-directed self-assembly of shape-controlled hydrogels. *Nature communications*, 4.
 - 17 Harikumar KG, Miller LJ. . (2009) Application of fluorescence resonance energy transfer techniques to establish ligand-receptor orientation. *Methods Mol Biol*; **552**:293-304. doi: 10.1007/978-1-60327-317-6_21. PubMed PMID: 19513658.
 - 18 Huang, J. S., Goh, T., Li, X., Sfeir, M. Y., Bielinski, E. A., Tomasulo, S., & Taylor, A. D. (2013). Polymer bulk heterojunction solar cells employing Forster resonance energy transfer. *Nature Photonics*, **7(6)**, 479-485.
 - 19 Kristoffersen AS, Erga SR, Hamre B, (2014) Frette Ø. Testing fluorescence lifetime standards using two-photon excitation and time-domain instrumentation: rhodamine B, coumarin 6 and lucifer yellow. *J Fluoresc*; **24(4)**:1015–1024. doi:10.1007/s10895-014-1368-1